

Measurement of properties of the Higgs boson decaying to pairs of W and Z bosons at 13 TeV with the CMS experiment

Muhammad Bilal Kiani^{*†}

Universita e INFN Torino (IT)

On the behalf of the CMS Collaboration

E-mail: muhammad.bilal.kiani@cern.ch

The properties of the Higgs boson are presented in the $H \rightarrow ZZ \rightarrow 4\ell$ ($\ell=e,\mu$) and $H \rightarrow WW \rightarrow e\nu\mu\nu$ decay channels using the data collected in Run2 of proton-proton collisions at a center-of-mass energy of 13 TeV recorded by the CMS detector at the LHC. The reported results include the signal-strength modifier μ , defined as the production cross section of the Higgs boson times its branching fraction relative to the standard model expectation, The signal-strength modifiers for the main Higgs boson production modes have also been constrained. The mass is measured to be $m_H = 125.26 \pm 0.21$ GeV and the width is constrained using on-shell production to be $\Gamma_H < 1.10$ GeV, at 95% CL. The fiducial cross section is measured to be $2.92_{-0.44}^{+0.48}(\text{stat.})_{-0.24}^{+0.28}(\text{sys.})$ fb, which is compatible with the standard model prediction.

The European Physical Society Conference on High Energy Physics

5-12 July

Venice, Italy

^{*}Speaker.

[†]A footnote may follow.

1. $H \rightarrow ZZ \rightarrow 4\ell$

The $H \rightarrow ZZ \rightarrow 4\ell$ decay channel ($\ell = e, \mu$) has a large signal-to-background ratio due to the complete reconstruction of the final state decay products and excellent lepton momentum resolution. This makes it one of the most important channels for studies of the Higgs boson's properties. Measurements performed using this decay channel and the Run 1 data set include the determination of the mass and spin-parity of the boson, its width and fiducial cross sections, as well as tests for anomalous HVV couplings explained in this paper [1].

The results are presented on the measurements of properties of the Higgs boson in the $H \rightarrow ZZ \rightarrow 4\ell$ decay channel at $\sqrt{s} = 13\text{TeV}$ using a data sample corresponding to an integrated luminosity of 35.9 fb^{-1} . Categories have been introduced targeting subleading production modes of the Higgs boson such as vector boson fusion (VBF) and associated production with a vector boson (WH, ZH) or top quark pair (ttH). In addition, dedicated measurements of mass and width of the boson and fiducial cross sections have been presented.

1.1 Analysis Strategy

To improve the sensitivity to the Higgs boson production mechanisms, the selected events are classified into mutually exclusive categories. Seven categories are defined, using the following criteria applied in this exact order. Figure 1 shows the signal relative purity of the seven event categories in several production processes.

The full kinematic information from each event using either the Higgs boson decay products or associated particles in its production is extracted using matrix element calculations and used to form several kinematic discriminants. The discriminant sensitive to $gg/q\bar{q} \rightarrow 4\ell$ kinematics is $\mathcal{D}_{\text{bkg}}^{\text{kin}}$ and the discriminants $\mathcal{D}_{1\text{jet}}, \mathcal{D}_{2\text{jet}}$ and $\mathcal{D}_{\text{VH}} = \max(\mathcal{D}_{\text{WH}}, \mathcal{D}_{\text{ZH}})$ are used to enhance the purity in event categories. The full definition of the observables can be found in Refs [2] [3] [4].

- **VBF-2jet-tagged category** exactly 4 leptons. In addition there must be either 2 or 3 jets of which at most 1 is b-tagged, or at least 4 jets and no b-tagged jets. Finally, $\mathcal{D}_{2\text{jet}} > 0.5$ is required.
- **VH-hadronic-tagged category** exactly 4 leptons. In addition there must be 2 or 3 jets, or at least 4 jets and no b-tagged jets. Finally, $\mathcal{D}_{\text{VH}} \equiv \max(\mathcal{D}_{\text{ZH}}, \mathcal{D}_{\text{WH}}) > 0.5$ is required.
- **VH-leptonic-tagged category** no more than 3 jets and no b-tagged jets in the event, and exactly 1 additional lepton or 1 additional pair of opposite sign same flavor leptons. This category also includes events with no jets and at least 1 additional lepton.
- **ttH-tagged category** at least 4 jets of which at least 1 is b-tagged, or at least 1 additional lepton.
- **VH-MET-tagged category** exactly 4 leptons, no more than 1 jet and $E_T^{\text{miss}} > 100\text{GeV}$.
- **VBF-1jet-tagged category** exactly 4 leptons, exactly 1 jet and $\mathcal{D}_{1\text{jet}} > 0.5$.
- **Untagged category** consists of the remaining events.

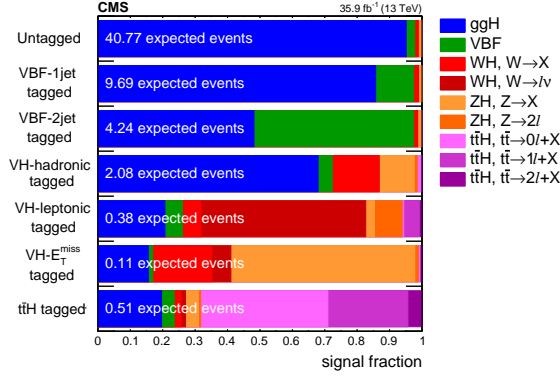


Figure 1: The signal relative purity of the seven event categories in terms of Higgs boson production processes in Ref [5].

1.2 Results

Signal Strength

To extract the signal strength modifier we perform a multi-dimensional fit that relies on two variables: the four-lepton invariant mass m_{4l} and the $\mathcal{D}_{\text{bkg}}^{\text{kin}}$ discriminant. We define the two-dimensional likelihood function as:

$$\mathcal{L}_{2D}(m_{4l}, \mathcal{D}_{\text{bkg}}^{\text{kin}}) = \mathcal{L}(m_{4l})\mathcal{L}(\mathcal{D}_{\text{bkg}}^{\text{kin}}|m_{4l}). \quad (1.1)$$

Figure 2 shows the results.

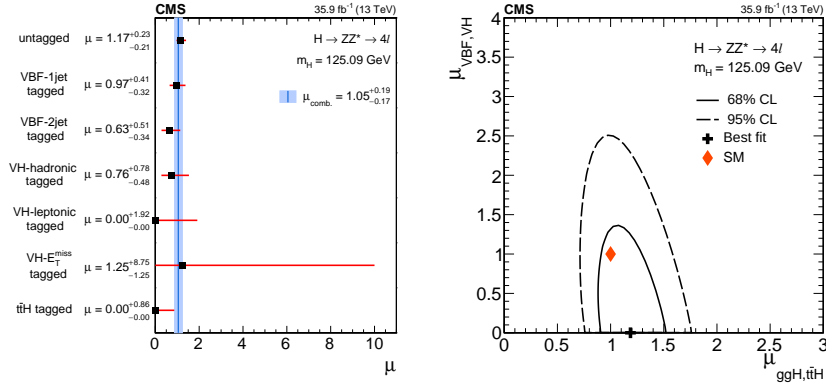


Figure 2: (Left): Observed values of the signal strength for the seven event categories, compared to the combined μ shown as a vertical line. (Right): Result of the 2D likelihood scan for the μ_F and μ_V signal strength modifiers. The solid and dashed contours show the 68% and 95% CL regions, respectively (Right) in Ref [5].

Fiducial Cross Section

The measurement of the cross section for the production and decay $pp \rightarrow H \rightarrow 4\ell$ within a fiducial volume defined to match closely the reconstruction level selection is presented. This measurement has minimal dependence on the assumptions of the relative fraction or kinematic distributions of the separate production modes. A maximum likelihood fit of the signal and background

parameterizations to the observed 4ℓ mass distribution, is performed to extract the integrated fiducial cross section without categorization and use of discriminants. See Figure 3 (Left).

Mass and Width

The measurement of the mass of the Higgs boson exploits additional information from per-event relative mass uncertainties $\mathcal{D}_{\text{mass}}$, which are defined by propagating per-lepton momentum errors to the 4ℓ candidate. Using this variable brings an expected improvement of about 8% to the uncertainty of the mass measurement, while the impact of also including $\mathcal{D}_{\text{bkg}}^{\text{kin}}$ is about 3%. Figure 3(Center) shows the results for 1D,2D and 3D likelihood scan. The nominal result is given by the 3D fit: $m_H = 125.26 \pm 0.20(\text{stat}) \pm 0.08(\text{sys.})$ GeV.

A measurement of the width performed using on-shell Higgs boson production. An unbinned maximum likelihood fit to the $m_{4\ell}$ distribution is performed over the range of selected events. The strength of fermion-induced couplings and vector-boson-induced couplings are independent and are left unconstrained in the fit. For such a large width, interference between the signal and background production of the $m_{4\ell}$ final state becomes important and is taken into account in analysis. Results shown in Figure 3 (Right).

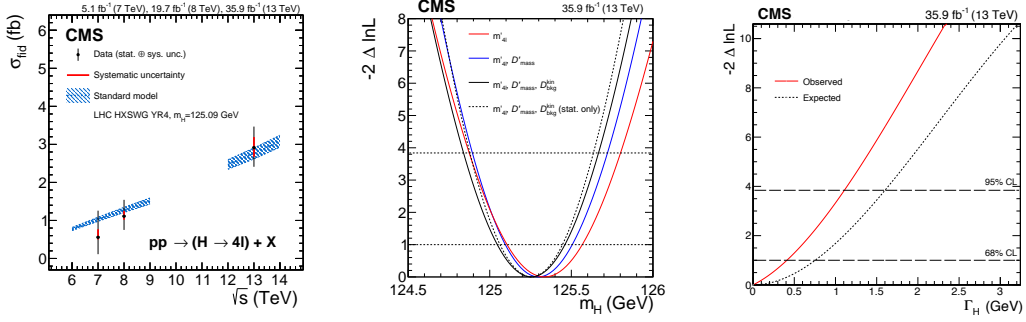


Figure 3: (Left): The measured fiducial cross section as a function of center of mass energy. (Center): likelihood scan as a function of mass for the 1D, 2D, and 3D measurement. (Right): Observed and expected likelihood scan of Γ_H using the signal range $105 < m_{4\ell} < 140$ GeV, with m_H floated in Ref [5].

2. $H \rightarrow WW \rightarrow e\nu\mu\nu$

The Higgs boson decay to a pair of W bosons was studied by the CMS experiment using the Run-I data set in leptonic final states exploring several production mechanisms, obtaining an excess significance of 4.3 standard deviations for a Higgs boson mass of 125.6 GeV [6].

The analysis presented here has final states in which the two W bosons decay leptonically are studied using data samples corresponding to an integrated luminosity of 15.2 fb^{-1} collected in RunII of LHC. Events with a pair of oppositely-charged leptons, namely one electron and one muon, missing transverse energy due to the presence of two neutrinos in the final state are selected. The main contribution comes from WW production, an irreducible background that shares the same final states and can only be separated by the use of certain kinematic properties. Background coming from top events ($t\bar{t}$ and single top tW) is also important, followed by other processes such as W+jets, Drell-Yan, and other electroweak productions. The analysis strategy follows closely the

one used during Run- I and in 2015 [6] in the same channel, extending to higher jet multiplicities to study VBF and VH production. For the associated production events with 3 leptons are also considered, targeting WH production.

2.1 Analysis Strategy

The main production mode for a Higgs boson at $m_H=125$ GeV is the gluon fusion mechanism for which extra jets in the final state arise only from parton initial or final state radiation. An analysis targeting gluon fusion then is mostly limited to events with no jets or, at maximum, one. In the WW decay mode of the Higgs boson, the fully leptonic final state is the cleanest to study and, from the leptonic decays, the opposite-flavor, $e\mu$ has the largest branching fraction and is the least affected by backgrounds. Therefore the analysis is performed selecting only $e^+\bar{\nu}_e\mu^-\nu_\mu$ and $e^-\nu_e\mu^+\bar{\nu}_\mu$ final states. However, the indirect contribution from τ leptons decaying leptonically is included. The neutrinos in the final state escape direct detection and lead to large missing transverse momentum in the events. Several background processes can lead to the same event properties and tight selection criteria are needed to enhance the sensitivity to the SM Higgs boson as detailed below.

The events are categorized according to the number of leptons, the number of jets, and the kinematics of the jets. The complete analysis strategy is summarized in the flowchart picture in Figure 4 and can be found at the reference [7].

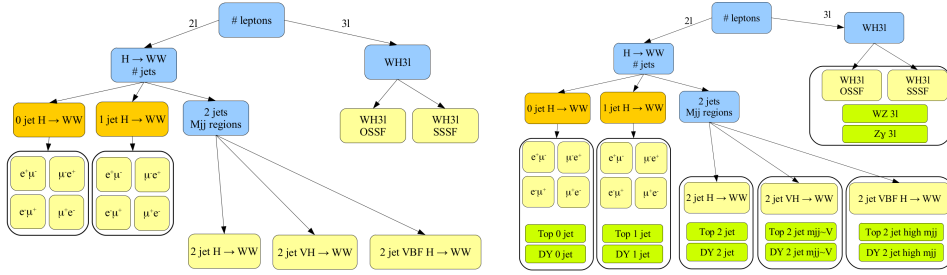


Figure 4: The flowchart of the analysis is reported here. (Left): without background control regions, on the right with the background control regions. The green boxes correspond to a separate cut based analyses used to control background normalization. The yellow boxes correspond to signal phase spaces for the analysis, and for each of them a template shape approach is followed in Ref [7].

To extract the Higgs boson signal in these categories, a similar strategy as in the Run-I analysis [6] is followed. Although the invariant mass of the Higgs boson can not be reconstructed due to the escaping neutrinos, the expected kinematic properties of the Higgs boson production and decay can be exploited. The spin 0 nature of the SM Higgs boson results in the emission of the two charged leptons close together. Moreover, the invariant mass of the two leptons in the signal is relatively small with respect to the one expected for a lepton pair arising from other processes such as non-resonant WW and top production. On the other hand, several of the smaller remaining backgrounds like fake leptons, $DY \rightarrow \tau\tau$, $V\gamma$ populate the same $m_{\ell\ell}$ phase space as the Higgs boson. These can be partially disentangled from the signal by reconstructing the Higgs boson transverse mass as

$$m_T = \sqrt{2p_T^{\ell\ell} E_T^{miss} (1 - \cos \Delta\phi(\ell\ell, \vec{E}_T^{miss}))},$$

where $\Delta\phi$ is the azimuthal angle between the di-lepton momentum and the MET. These additional backgrounds populate different regions of the two dimensional plane in $m_{\ell\ell}$ and m_T .

2.2 Results

In order to visualize the final results in the most performing categories, a weighted plot of $m_{\ell\ell}$ has been produced, and shown in Figure 5. For each window in m_T^H and for each category and data taking period, a weight is calculated as the ratio of the expected signal to the sum of background events. The different $m_{\ell\ell}$ distributions in windows in m_T^H , and for each category, are then summed and normalized to the expected total signal yield. The same procedure is performed on data and on MC distributions, and the background subtracted data distributions are shown as well in Figure 5 (right), where the red line is the expected signal distribution: the observed distributions show good agreement with the expected Higgs boson distributions.

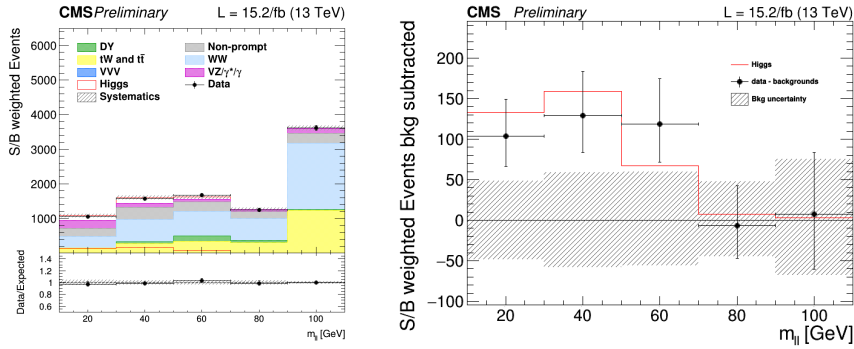


Figure 5: (Left): The weighted distribution, (Right): the background subtracted distribution in Ref [7].

The final binned fit is performed using template histograms for all signal and background processes obtained after all selection criteria explained in the Reference [7]. Observed (and expected) significance and signal strength for the SM Higgs boson with a mass of 125 GeV for all the categories is shown in table below 6 Left. Also the likelihood scan on the signal strength for gluon fusion and VBF/VH, including one and two σ contours are shown in the Figure 6 (Right).

category	significance	σ/σ_{SM}
0-jet	2.7 (2.9)	$0.9^{+0.4}_{-0.3}$
1-jet	2.1 (2.5)	$1.1^{+0.4}_{-0.4}$
2-jet	2.0 (1.0)	$1.3^{+1.0}_{-1.0}$
VBF 2-jet	2.2 (1.5)	$1.4^{+0.8}_{-0.8}$
VH 2-jet	1.0 (0.4)	$2.1^{+2.3}_{-2.2}$
WH 3-lep	0.0 (0.5)	$-1.4^{+1.5}_{-1.5}$
combination	4.3 (4.1)	$1.05^{+0.27}_{-0.25}$

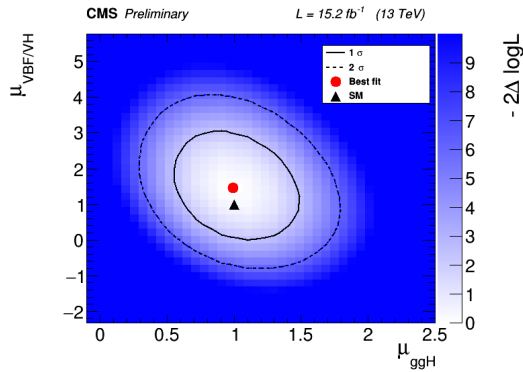


Figure 6: (Left): Observed (and expected) significance and signal strength for the SM Higgs boson with a mass of 125 GeV for all the categories. (Right): Likelihood scan on the signal strength for gluon fusion and VBF/VH in Ref [7].

3. Conclusions

Several measurements of Higgs boson production in the four-lepton final state at $\sqrt{s} = 13\text{TeV}$ have been presented, using data samples corresponding to an integrated luminosity of 35.9fb^{-1} for $H \rightarrow ZZ \rightarrow 4\ell$ and 15.2fb^{-1} for $H \rightarrow WW \rightarrow 2\ell 2\nu$. All results are consistent, within their uncertainties, with the expectations for the SM Higgs boson. The detailed analysis is explained in [8] for $H \rightarrow ZZ \rightarrow 4\ell$.

References

- [1] S. Chatrchyan *et al.* [CMS Collaboration], Phys. Rev. D **89**, 0920007 (2013) [arXiv:1312.5353 [hep-ex]].
- [2] V. Khachatryan *et al.* [CMS Collaboration], Phys. Rev. D **92**, 012004, (2015) [arXiv:1411.3441 [hep-ex]].
- [3] Y. Gao *et al.* [CMS Collaboration], Phys. Rev. D **81**, 075022, (2010) [arXiv:1001.3396 [hep-ex]].
- [4] S. Bolognesi *et al.* [CMS Collaboration], Phys. Rev. D **86**, 095031, (2012) [arXiv:1208.4018 [hep-ex]].
- [5] A. Sirunyan *et al.* [CMS Collaboration], Submitted to JHEP (2017) [arXiv:1706.09936 [hep-ex]].
- [6] S. Chatrchyan *et al.* [CMS Collaboration], JHEP **1401**, 096, (2014) [arXiv:1312.1129 [hep-ex]].
- [7] [CMS Collaboration], CMS-PAS-HIG-16-021, 2017, <https://cds.cern.ch/record/2273908>.
- [8] Sirunyan, Albert M *et al.* [CMS Collaboration], [arXiv:1706.09936 [hep-ex]]